Supporting Information for the Manuscript Entitled

Mechanism underlying the effectiveness of deferiprone in alleviating Parkinson's disease symptoms

Yingying Sun, An Ninh Pham and T. David Waite*

School of Civil and Environmental Engineering, The University of New South Wales, Sydney, NSW 2052, Australia

Keywords: Deferiprone, Iron overload, Dopamine, Parkinson's disease, Mechanism and Oxidative stress

ACS Chemical Neuroscience

* Corresponding author. Professor T. David Waite, Tel.: +61 2 9385 5059, Email: d.waite@unsw.edu.au

SI 1 Equilibrium calculation for the Fe-DA complexes

Generally, all the forms of DFP (including $HDFP^0$ and DFP^-) can form complexes with iron. The stability constants listed in Table S4 is the one between iron and DFP^-. In the presence of $HDFP^0$, the associated stability constant for the equilibrium would change accordingly for the participation of H^+. An example is shown below for the calculation of stability constant between Fe(III) and $HDFP^0$.

For the equilibrium between $Fe^{3+} + HDFP^0 \rightleftharpoons FeDFP^{2+} + H^+$, the stability constant K^* can be written as follows:

$$K^* = \frac{[FeDFP^{2+}][H^+]}{[Fe^{3+}][HDFP^0]} = \frac{[FeDFP^{2+}]}{[Fe^{3+}][DFP^-]} \bullet \frac{[DFP^-][H^+]}{[HDFP^0]} = K \bullet K_{a2} \qquad \text{S1}$$

As such, $\text{Log}K^*$ can be calculated as 6.04 by using the stability constant listed in Table S4. The definition of stability constant is

$$K = \frac{k_+}{k_-} \qquad \text{S2}$$

where k_+ and k_- are the associated formation and dissociation rate constant.[1] Thus, for a given formation rate constant, the corresponding dissociation rate constant can be calculated as k_+/K. Even though $HDFP^0$ is the dominant DFP species at the physiological pH 7.4 investigated in this study, proportional increase in the concentrations of the much more active DFP^- as a result of the increase in total DFP concentrations would definitely decrease the apparent dissociation rate constant.

SI 2 Model revision and justification

Revised model for the interaction between iron and DA

Table S1 Modelled reactions and rate constants for the autoxidation of DA at pH 7.4

No.	Reactions	Rate constants ($M^{-1}s^{-1}$ or s^{-1})	Reference
1	$DA + O_2 \xrightarrow{k_1} O_2^{\bullet-} + DA^{\bullet-}$	$k_1 = 8.24 \times 10^{-3}$ [a]	This study
2	$DA^{\bullet-} + O_2 \underset{k_{-2}}{\overset{k_2}{\rightleftharpoons}} DAQ + O_2^{\bullet-}$	$k_2 = 2.95 \times 10^3$	1
		$k_{-2} = 1.0 \times 10^9$	1
3	$DA^{\bullet-} + DA^{\bullet-} \xrightarrow{k_3} DA + DAQ$	$k_3 = 2.35 \times 10^8$	2
4	$DAQ \xrightarrow{k_4} DAL$	$k_4 = 4.45$ [a]	This study
5	$DAL + DAQ \xrightarrow{k_5} DA + DAC$	$k_5 = 5.30 \times 10^6$	3
6	$DAL + O_2 \xrightarrow{k_6} DAC + H_2O_2$	$k_6 = 5.12$ [a]	This study
7	$O_2^{\bullet-} + O_2^{\bullet-} \xrightarrow{k_7} H_2O_2 + O_2$	$k_7 = 1.9 \times 10^5$	4
8	$DA^{\bullet-} + O_2^{\bullet-} \xrightarrow{k_8} DAQ + H_2O_2$	$k_8 = 8.27 \times 10^9$ [b]	5

Note: a: modified value for the model developed at pH 7.4 in Sun et al. [2];
b: rate constant taken from Sun et al. [2] without modification;
DA, dopamine; $DA^{\bullet-}$, dopamine semiquinone radical; DAQ, DA *o*-quinone; DAC, aminochrome; DAL, leukoaminochrome and $O_2^{\bullet-}$, superoxide
(1) Pham and Waite [3]; (2) Borovansky et al. [4]; (3) Land et al. [5]; (4) Zafiriou [6] and (5) Sun et al. [2].

Table S2 Modelled reactions and rate constants for Fe(III)-catalyzed oxidation of DA at pH 7.4

No.	Reactions	Rate constants ($M^{-1}s^{-1}$ or s^{-1})	Reference
9	$Fe(III) + Fe(III)_I \xrightarrow{k_9} AFO + nH^+$	$k_9 = 5.0 \times 10^6$	6
10	$>Fe(III)_n + DA \xrightarrow{k_{10}} >Fe(III)_{n-1} + Fe^{III}DA$	$k_{10} = 2.34$ [b]	5
11	$>Fe(III)_n + DA \xrightarrow{k_{11}} >Fe(III)_{n-1} + Fe(II) + DA^{\bullet-}$	$k_{11} = 0.6$ [b]	5
12	$Fe(III) + DA \underset{k_{-12}}{\overset{k_{12}}{\rightleftharpoons}} Fe^{III}DA$	$k_{12} = 4.15 \times 10^5$ [a] $k_{-12} = 0.46$	This study This study
13	$Fe^{III}DA + DA \underset{k_{-13}}{\overset{k_{13}}{\rightleftharpoons}} Fe^{III}DA_2$	$k_{13} = 4.5 \times 10^5$ $k_{-13} = 2.59 \times 10^{-4}$	7 This study
14	$Fe^{III}DA + O_2^{\bullet-} \xrightarrow{k_{14}} Fe^{II}DA + O_2$	$k_{14} = 1.5 \times 10^8$ [b]	5
15	$Fe^{III}DA \xrightarrow{k_{15}} Fe(II) + DA^{\bullet-}$	$k_{15} = 0.23$	8
16	$Fe^{III}DA_2 \xrightarrow{k_{16}} Fe(II) + DA + DA^{\bullet-}$	$k_{16} = 7.26 \times 10^{-5}$ [b]	5
17	$Fe(III) + O_2^{\bullet-} \underset{k_{-17}}{\overset{k_{17}}{\rightleftharpoons}} Fe(II) + O_2$	$k_{17} = 1.5 \times 10^8$ $k_{-17} = 0.77$ [b]	9 5
18	$>Fe(III)_n + O_2^{\bullet-} \xrightarrow{k_{18}} >Fe(III)_{n-1} + Fe(II) + O_2$	$k_{18} = 3.7 \times 10^5$ [b]	5

Note: a: modified value for the model developed at pH 7.4 in Sun et al. [2];
b: rate constant taken from Sun et al. [2] without modification.

DA, dopamine; $DA^{\bullet-}$, dopamine semiquinone radical; $O_2^{\bullet-}$, superoxide; Fe(III), inorganic ferric ion; $Fe(III)_I$, total inorganic Fe(III); AFO, ferrihydrite and Fe(II), inorganic ferrous ion
(6) Pham et al. [7]; (7) Blesa and Matijević [8]; (8) El-Avaan et al. [9] and (9) Rush and Bielski [10].

Table S3 Modelled reactions and rate constants for Fe(II)-catalyzed oxidation of DA at pH 7.4

No.	Reactions	Rate constants ($M^{-1}s^{-1}$ or s^{-1})	Reference
19	$Fe(II) + O_2^{\bullet-} \xrightarrow{k_{19}} Fe(III) + H_2O_2$	$k_{19} = 1 \times 10^7$	9
20	$Fe(II) + H_2O_2 \xrightarrow{k_{20}} Fe(III) + {}^{\bullet}OH + OH^-$	$k_{20} = 1.33 \times 10^4$	10
21	$Fe(II) + DA \underset{k_{-21}}{\overset{k_{21}}{\rightleftharpoons}} Fe^{II}DA$	$k_{21} = 7.5 \times 10^{2}$ [b]	5
		$k_{-21} = 1.6 \times 10^{-3}$	This study
22	$Fe^{II}DA + O_2 \xrightarrow{k_{22}} Fe^{III}DA + O_2^{\bullet-}$	$k_{22} = 1.45 \times 10^{2}$ [b]	5
23	$Fe^{II}DA + H_2O_2 \xrightarrow{k_{23}} Fe^{III}DA + {}^{\bullet}OH + OH^-$	$k_{23} = 1.33 \times 10^4$	10
24	$Fe^{II}DA + O_2^{\bullet-} \xrightarrow{k_{24}} Fe^{III}DA + H_2O_2$	$k_{24} = 1 \times 10^{7}$ [b]	5
25	$Fe^{II}DA + DA^{\bullet-} \xrightarrow{k_{25}} Fe^{III}DA + DA$	$k_{25} = 1.92 \times 10^{5}$ [b]	5

Note: a: modified value for the model developed at pH 7.4 in Sun et al. [2];
b: rate constant taken from Sun et al. [2] without modification.

DA, dopamine; $DA^{\bullet-}$, dopamine semiquinone radical; $O_2^{\bullet-}$, superoxide; Fe(III), inorganic ferric ion; Fe(II), inorganic ferrous ion; H_2O_2, peroxide and ${}^{\bullet}OH$, hydroxyl radicals
(10) González-Davila et al. [11].

Model justification for impact of DFP on the transformation of iron both in the absence and presence of DA

To better constrain and understand the key processes of the complicated model developed in Tables 1 – 3 (main text), several intermediates were measured in this study. Briefly, i) the formation of $Fe^{III}DFP_3$ complexes (Figure 1) is used for the constraint of the competition between the chelation and precipitation of aqueous Fe(III); ii) the decay of Fe(II) coupled with the formation $Fe^{III}DFP_3$ and H_2O_2 are used to constrain the transformation of Fe(II) in the presence of DFP (Figure 2); iii) the formation H_2O_2 shown in Figure 4 is used for the investigation of the radicals mediated processes, including the transformation of $O_2^{\bullet-}$ and $DA^{\bullet-}$; iv) the ligand exchange between DA and DFP under deoxygenated condition is used for the investigation of the efficiency of DFP to overcome the thermodynamic barrier and scavenging the loosely DA bound iron (Figure 3). Discussion of factors underpinning the selection of rate constants shown in Tables 1 – 3 is provided below. The sensitivity analysis is used herein to determine the relative importance of the proposed reactions. Specifically, the more variation of the relative residual *r* to the change in the orders of magnitude of the rate constant, the more important the reaction is and the lowest point is generally considered to be the optimal rate constant of this reaction.

As shown in Figure S1a, in general, chelation of aqueous Fe(III) is important processes since the relative residual *r* of each reaction is sensitive to the change in the orders of magnitude of rate constant. Consistently, shift points in Figure S1a are evident at the proposed values in the main text, which indicate that the proposed values should be the optimal values in view of aqueous ferric iron chelation by DFP. Compared with the previous proposed values (shown in Table S2) for another bidentate chelator, DA, the much larger rate constants for the formation of *mono*-complex and coordinated H_2O replacement process proposed herein for DFP may mainly attribute to the enhanced proportion of the deprotonated phenol groups as a result of the lower pK_a values of DFP than that of DA. In general, the replacement of a coordinated H_2O by another organic molecule is generally faster than the formation of the *mono*-complex.[12] From the point, the rate constants (1.16×10^8 $M^{-1}s^{-1}$)

proposed for the formation of *bis*- and *tris*-complexes from $Fe^{III}DFP$ and $Fe^{III}DFP_2$ with another DFP (reactions 3 and 4 in Table 1) is reasonable. However, in comparison with the water-loss rate of $Fe(OH)(H_2O)_5^{2+}$ (4.50×10^5 $M^{-1}s^{-1}$) [8] used for the formation of the $Fe^{III}DA_2$ complex, the two orders of magnitude greater rate constants used for DFP may result from the enhanced electrostatic attraction force between the positively charged iron and negatively charged DFP as well as the influence of DFP as a strong field ligand. Compared with the sensitive values for the chelation of aqueous iron, the rate constant proposed for the iron mobilization by DFP can only be treated as the upper limit value as a result of the generally insensitivity of the relative residual *r* to the change in the rate constant below the proposed value.

Similar to the formation of Fe(III)-DFP complexes, dissociation of these complexes is also of great significance for the considerable sensitivity of relative residual *r* to the change in the rate constant over several orders of magnitude (shown in Figure S1b). In general, the proposed dissociation rate constants are consistent with the calculated optimal values herein. As shown in Figure S1b, it is evident that the optimal rate constants of the dissociation process increase significantly on the decrease in the coordinated numbers of DFP, which is consistent with the commonly recognized fact that the complexes formed with more ligands are generally much more stable.

As shown in Figure S1c, in consistent with the situation of Fe(III), formation and dissociation of *mono*-complex between Fe(II) and DFP is of great importance for its considerable sensitivity of the relative residual *r* to the change in the rate constant over several orders of magnitude. The shift points in Figure S1c are converged at the proposed values in the main text, which indicates that the proposed values should be the optimal values.

As shown in Figure S1d, in view of the DFP induced scavenging of Fe(II), the oxidation of DFP bound Fe(II) by O_2 should be the dominant pathway for the considerable sensitivity of the relative residual *r* of this process to the change in the rate constant over several orders of magnitude.

This is reasonable by taking into account the concentrations of different oxidant and rate constants of each process in view of the rate law. In specific, in the air-saturated solutions investigated herein, the concentration of O_2 is around 243 μM, while the concentrations of H_2O_2 and $O_2^{\bullet-}$ is only at nanomole and sub-nanomole range and should be even lower *in vivo* as a result of the mature antioxidant system. As such, it is unexpected that $k_{Fe^{II}DFP+O_2}[Fe^{II}DFP][O_2]$ should be much larger than that of $k_{Fe^{II}DFP+H_2O_2}[Fe^{II}DFP][H_2O_2]$ and $k_{Fe^{II}DFP+O_2^{\bullet-}}[Fe^{II}DFP][O_2^{\bullet-}]$.

As shown in Figure S1e, compared with the reduction of $DFP^{\bullet-}$ by $O_2^{\bullet-}$, the oxidation of DFP by $DA^{\bullet-}$ is a much more important process for the sensitivity of the relative residual *r* of this process to the change in the rate constant over several orders of magnitude. The generally consistence of the proposed rate constant with the shift point shown in Figure S1e indicates that the proposed value should be the optimal rate constant. In contrast, the generally insensitivity of the rate constant of reduction of $DFP^{\bullet-}$ by $O_2^{\bullet-}$ may suggest that the rate constant proposed herein may only be a lower limit of this process.

As shown in Figure S1f, the relative residual *r* of the ligand exchange process between $Fe^{III}DA$ and DFP is not as sensitive as the one between DFP and $Fe^{III}DA_2$. As such, to simplify the complicated model, the ligand exchange between $Fe^{III}DA$ and DFP is not included in the model. Indeed, the insensitivity of this process may mainly result from the extremely low concentrations of $Fe^{III}DA$ species under physiological condition investigated herein. For the generally insensitivity of relative residual *r* to the change in the rate constant of ligand exchange process of $Fe^{III}DA_2$ and DFP during the range $10^3 \sim 10^7$ $M^{-1}s^{-1}$, the proposed rate constants in this study may only be the upper limits of this process. The consistence with the formation rate constants proposed for the organics induced ferric complexation in open oceans [13] coupled with same order of the rate constants of the DFP induced chelation of aqueous and DA bound Fe(III) indicates that the proposed values herein should be reasonable.

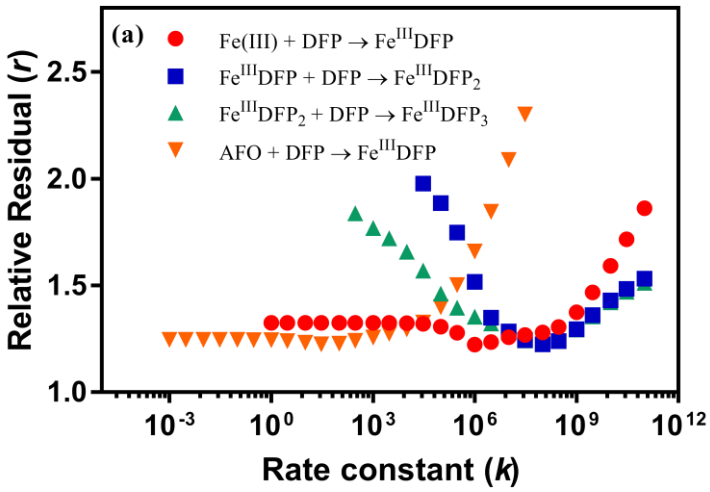
(a)
Fe(III) + DFP → Fe^III DFP
Fe^III DFP + DFP → Fe^III DFP2
Fe^III DFP2 + DFP → Fe^III DFP3
AFO + DFP → Fe^III DFP
Relative Residual (r)
2.5
2.0
1.5
1.0
10-3
100
103
106
109
1012
Rate constant (k)

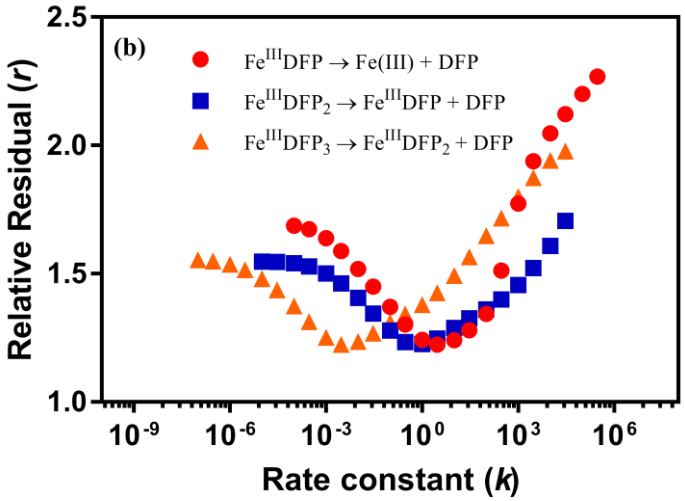
(b)
Fe^III DFP → Fe(III) + DFP
Fe^III DFP2 → Fe^III DFP + DFP
Fe^III DFP3 → Fe^III DFP2 + DFP
Relative Residual (r)
2.5
2.0
1.5
1.0
10-9
10-6
10-3
100
103
106
Rate constant (k)

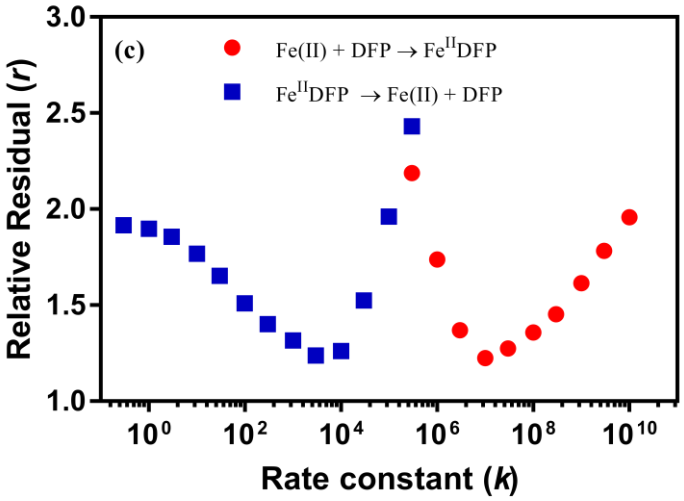
(c)
Fe(II) + DFP → Fe^IIDFP
Fe^IIDFP → Fe(II) + DFP
Relative Residual (r)
3.0
2.5
2.0
1.5
1.0
10^0
10^2
10^4
10^6
10^8
10^10
Rate constant (k)

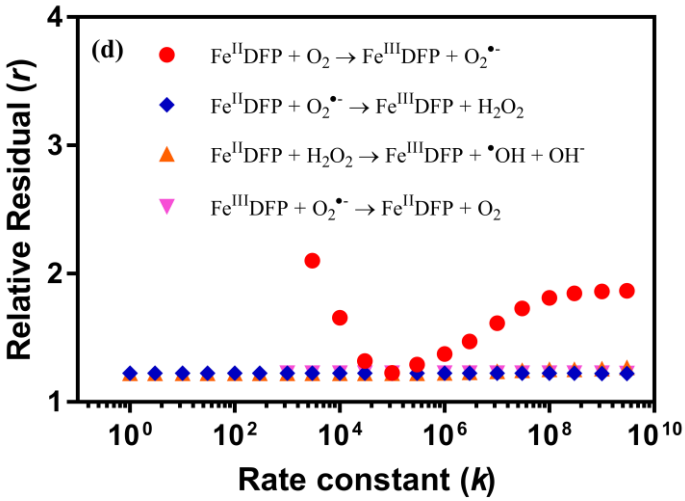
(d)
Fe^IIDFP + O2 → Fe^IIIDFP + O2•-
Fe^IIDFP + O2•- → Fe^IIIDFP + H2O2
Fe^IIDFP + H2O2 → Fe^IIIDFP + •OH + OH-
Fe^IIIDFP + O2•- → Fe^IIDFP + O2
Relative Residual (r)
4
3
2
1
10^0
10^2
10^4
10^6
10^8
10^10
Rate constant (k)

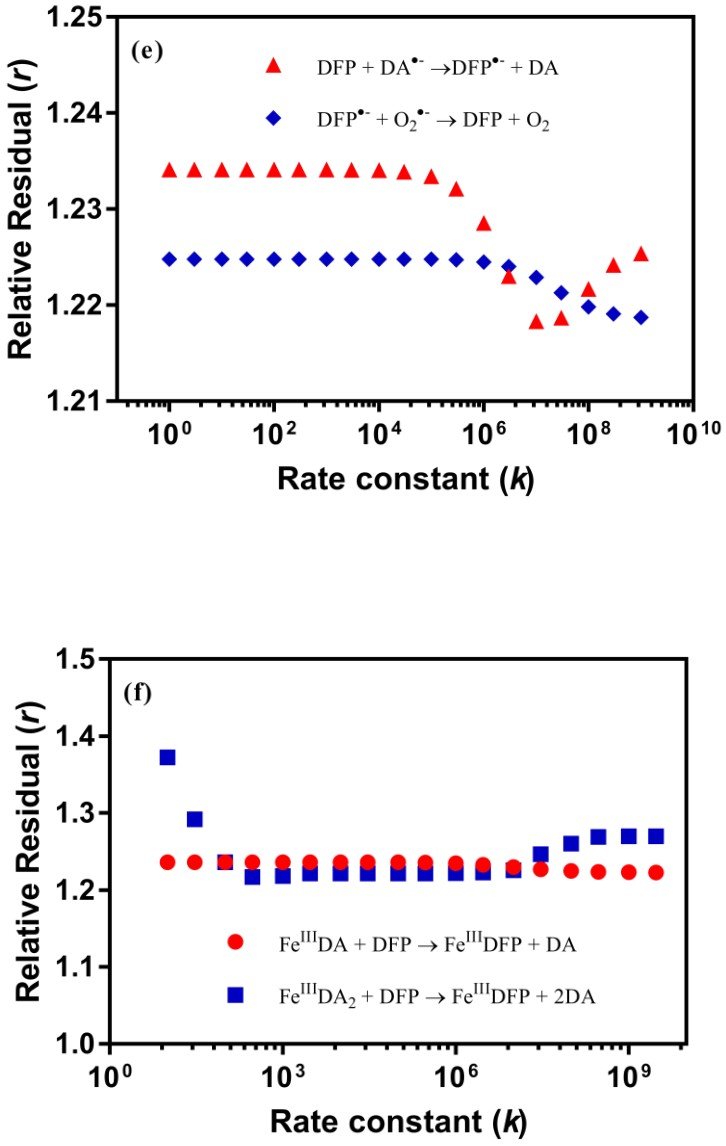

Figure S1. Sensitivity analysis for the fitted rate constants of different reactions (Tables 1 - 3, main text).

SI 3 Speciation of Fe(III)/Fe(II)-DFP complexes

Stability constants for Fe(II) and Fe(III) speciations

Table S4. Stability constants for Fe(II) and Fe(III) speciations at 25 ℃ and I = 0.

No.	species	Log$K$	Reference
Fe(II) species			
1	$Fe^{2+} + H_2O \rightleftharpoons FeOH^+ + H^+$	-9.51	1
2	$Fe^{2+} + 2H_2O \rightleftharpoons Fe(OH)_2^0 + 2H^+$	-20.6	1
3	$Fe^{2+} + CO_3^{2-} \rightleftharpoons FeCO_3^0$	5.69	2
4	$Fe^{2+} + H^+ + CO_3^{2-} \rightleftharpoons FeHCO_3^+$	11.8	3
5	$Fe^{2+} + 2CO_3^{2-} \rightleftharpoons Fe(CO_3)_2^{2-}$	7.45	2
6	$Fe^{2+} + CO_3^{2-} + H_2O \rightleftharpoons Fe(OH)CO_3^- + H^+$	-4.03	2
7	$Fe^{2+} + Cl^- \rightleftharpoons FeCl^+$	0.3	2
8	$Fe^{2+} + SO_4^{2-} \rightleftharpoons FeSO_4^0$	2.42	2
9	$Fe^{2+} + DA^{2-} \rightleftharpoons FeDA^0$	9.12	4
10	$Fe^{2+} + 2DA^{2-} \rightleftharpoons FeDA_2^{2-}$	14.56	4
11	$Fe^{2+} + DFP^- \rightleftharpoons FeDFP^+$	5.67	5
12	$Fe^{2+} + 2DFP^- \rightleftharpoons Fe(DFP)_2^0$	9.65	5
13	$Fe^{2+} + 3DFP^- \rightleftharpoons Fe(DFP)_3^-$	13.06	6
Fe(III) species			
14	$Fe^{3+} + H_2O \rightleftharpoons Fe(OH)^{2+} + H^+$	-2.13	7
15	$Fe^{3+} + 2H_2O \rightleftharpoons Fe(OH)_2^+ + 2H^+$	-6.13	7
16	$Fe^{3+} + 3H_2O \rightleftharpoons Fe(OH)_3^0 + 3H^+$	-14.3	7
17	$Fe^{3+} + 4H_2O \rightleftharpoons Fe(OH)_4^- + 4H^+$	-22.2	7
18	$Fe^{3+} + Cl^- \rightleftharpoons FeCl^{2+}$	1.28	7
19	$Fe^{3+} + 2Cl^- \rightleftharpoons FeCl_2^+$	1.16	7
20	$Fe^{3+} + SO_4^{2-} \rightleftharpoons Fe(SO_4)^+$	4.27	7

21	$Fe^{3+} + 2SO_4^{2-} \rightleftharpoons Fe(SO_4)_2^-$	6.11	7
22	$Fe^{3+} + 2CO_3^{2-} \rightleftharpoons Fe(CO_3)_2^-$	19.6	7
23	$Fe^{3+} + DA^{2-} \rightleftharpoons FeDA^+$	21.42	8
24	$Fe^{3+} + 2DA^{2-} \rightleftharpoons FeDA_2^-$	36.46	8
25	$Fe^{3+} + 3DA^{2-} \rightleftharpoons FeDA_3^{3-}$	45.08	8
26	$Fe^{3+} + DFP^- \rightleftharpoons FeDFP^{2+}$	15.80	9
27	$Fe^{3+} + 2DFP^- \rightleftharpoons Fe(DFP)_2^+$	27.78	9
28	$Fe^{3+} + 3DFP^- \rightleftharpoons Fe(DFP)_3^0$	37.25	9
Aqueous species			
29	$H^+ + OH^- \rightleftharpoons H_2O$	14	10
30	$H^+ + CO_3^{2-} \rightleftharpoons HCO_3^-$	10.3	10
31	$2H^+ + CO_3^{2-} \rightleftharpoons H_2CO_3^*$	16.7	10
32	$NH_3 + H^+ \rightleftharpoons NH_4^+$	9.24	1
33	$H^+ + SO_4^{2-} \rightleftharpoons HSO_4^-$	1.99	1
34	$Na^+ + CO_3^{2-} \rightleftharpoons NaCO_3^-$	1.27	2
35	$Na^+ + H^+ + CO_3^{2-} \rightleftharpoons NaHCO_3^0$	10.1	2
36	$Na^+ + SO_4^{2-} \rightleftharpoons NaSO_4^-$	1.06	2
37	$NH_4^+ + SO_4^{2-} \rightleftharpoons NH_4SO_4^-$	1.03	11
38	$H_2DA \rightleftharpoons HDA^- + H^+$	-10.58	12
39	$HDA^- \rightleftharpoons DA^{2-} + H^+$	-12.07	12
40	$H_2DFP^+ \rightleftharpoons HDFP + H^+$	-3.62	9
41	$HDFP \rightleftharpoons DFP^- + H^+$	-9.76	9

Note: the ratio of stability constant β_3/β_2 and β_3/β_1 of DFP for Fe(II) was assumed to be similar to those for Fe(III) since β_1 and β_2 are not unknown.

(1) Morel and Hering [1]; (2) King [14]; (3) Millero and Hawke [15]; (4) Smith and Martell [16]; (5) Merkofer et al. [17]; (6) Merkofer et al. [18]; (7) Pham et al. [7]; (8) Avdeef et al. [19]; (9) Motekaitis and Martell [20]; (10) Millero et al. [21]; (11) Schecher and McAvoy [22] and (12) Pham and Waite [3]

Distribution of DFP and Fe(III)–DFP complexes

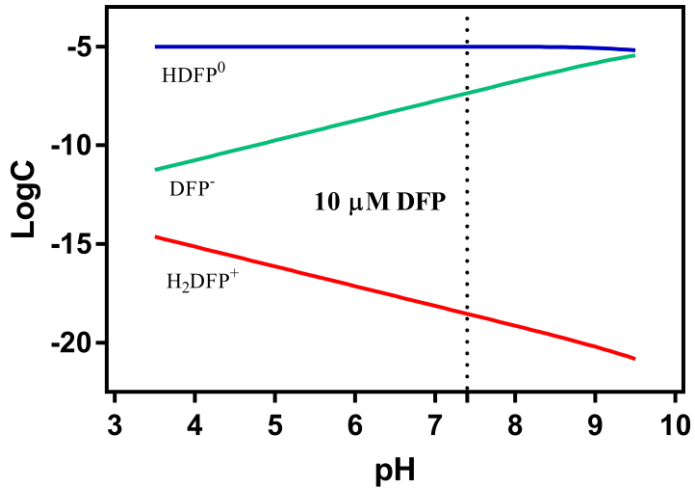

Figure S2 Distribution of DFP species over a range of pH. The dashed line corresponds to the Log concentration of different species at pH 7.4.

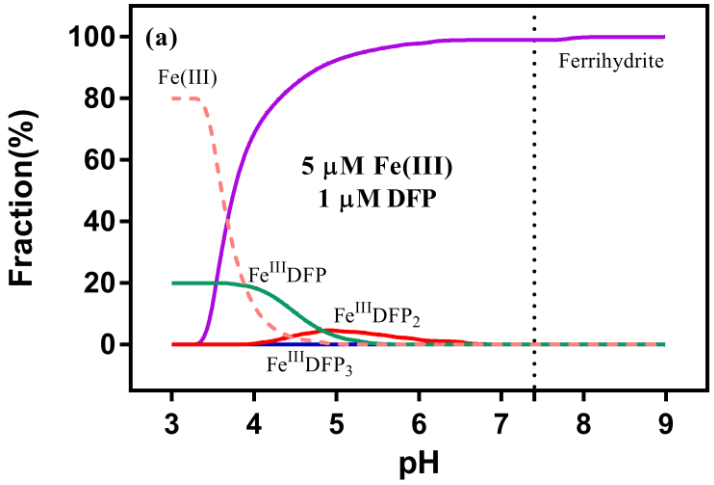

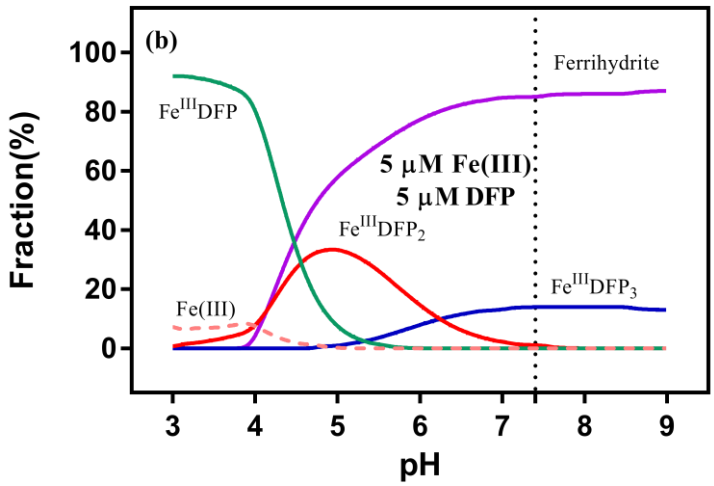
(b)
Ferrihydrite
Fe^{III}DFP
5 μM Fe(III)
5 μM DFP
Fe^{III}DFP$_2$
Fe^{III}DFP$_3$
Fe(III)
Fraction(%)
pH

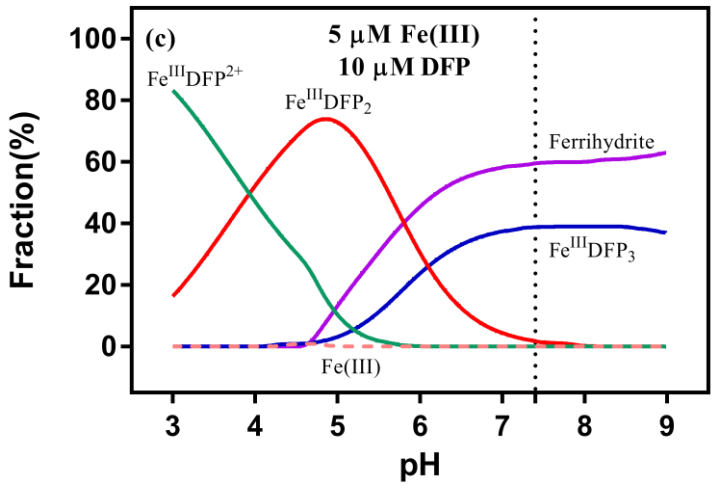
(c)
5 μM Fe(III)
10 μM DFP
Fe^{III}DFP^{2+}
Fe^{III}DFP$_2$
Ferrihydrite
Fe^{III}DFP$_3$
Fe(III)
Fraction(%)
pH

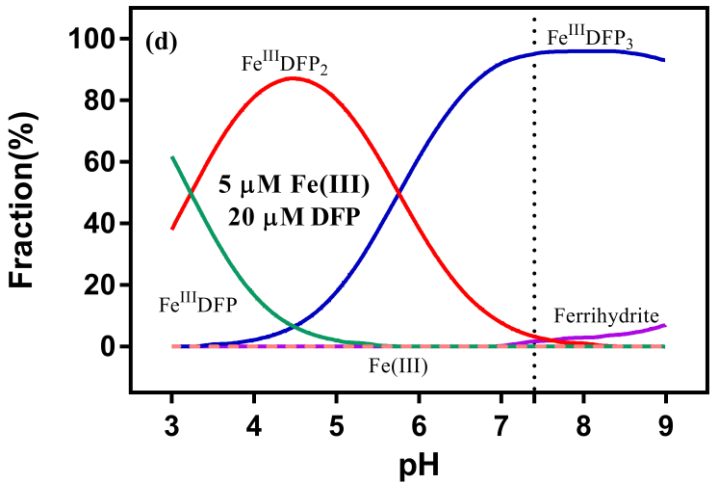
(d)
Fe^{III}DFP$_3$
Fe^{III}DFP$_2$
5 μM Fe(III)
20 μM DFP
Fe^{III}DFP
Ferrihydrite
Fe(III)
Fraction(%)
pH

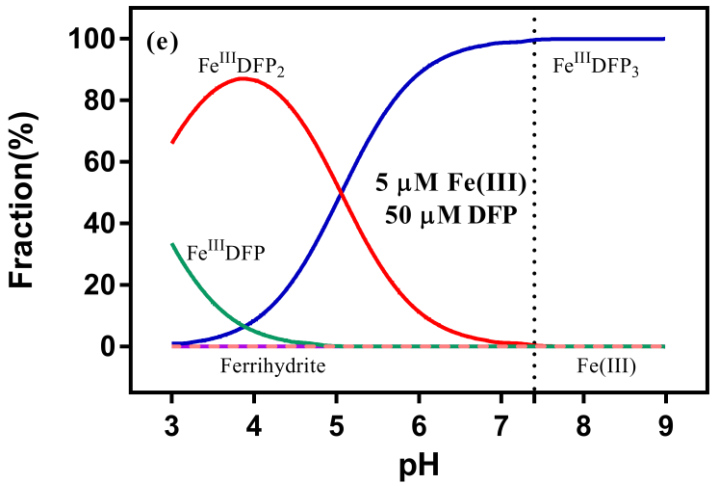

Figure S3 Distribution of Fe(III)-DFP complexes in the presence of different [DFP]/[Fe(III)] ratios over a range of pH. The dashed line corresponds to the fraction values of different species at pH 7.4. Fe(III) represents the total concentration of inorganic ferric ion.

SI 4 Relative importance of DFP autoxidation and iron-catalyzed DFP oxidation

Generally, in the presence of O_2, despite being thermodynamically unfavorable and spin forbidden, organic compounds tend to be oxidized, resulting in the generation of H_2O_2. The rate of this process varies significantly as a result of the discrepancy in chemical properties.[2, 23] The generated H_2O_2 may be a potential risk for the participation in the Fenton reaction sequence in the presence of Fe(II) to generate the much more powerful $^{\bullet}OH$.

Interestingly, in contrast to previous work,[2] negligible accumulations of H_2O_2 can be measured over 1 hour oxidation (Figure S4a). The concentrations of H_2O_2 generated during this process even decreased slightly on increase in DFP concentration and, were almost stable over the 1-hour experiments. This phenomenon might be due to the specific nature of this compound. In particular, the -N substitute may significantly decrease the electron density on the hard O donors in the phenol functional groups through the electron withdrawing effect for its strong electronegativity. As a consequence, the organic molecules may become more reluctant to be oxidized.

Normally, the oxidation of organic substance can be accelerated in the presence of transition metals[24] with resultant in the enhanced accumulation of H_2O_2. However, in the presence of Fe(III), the concentrations of H_2O_2 generated from the oxidation of DFP was even slightly lowered (Figure S4b).

In order to further verify the possibility of the interaction between H_2O_2 and Fe(III)-DFP complexes, 1 μM H_2O_2 was added to the 5 μM Fe(III) and 10 μM DFP containing solutions. As shown in Figure S4c, negligible decay of H_2O_2 can be observed over 1-hour reaction. As such, in this study, we assumed that direct reaction between Fe(III)-DFP and H_2O_2 is not important or is not the dominant decay pathway of H_2O_2. In general, even though it has been reported that Fe(III) could react directly with H_2O_2, the rate constant of this reaction is several orders of magnitude smaller than is the case of Fe(II).[25]

Given the experimental data, we assume that the autoxidation and iron-catalyzed oxidation of DFP was negligible. In order to simplify the complicated kinetic model developed in this work, these two reactions were treated as unimportant pathways and were not included in the model proposed in Tables 1 – 3.

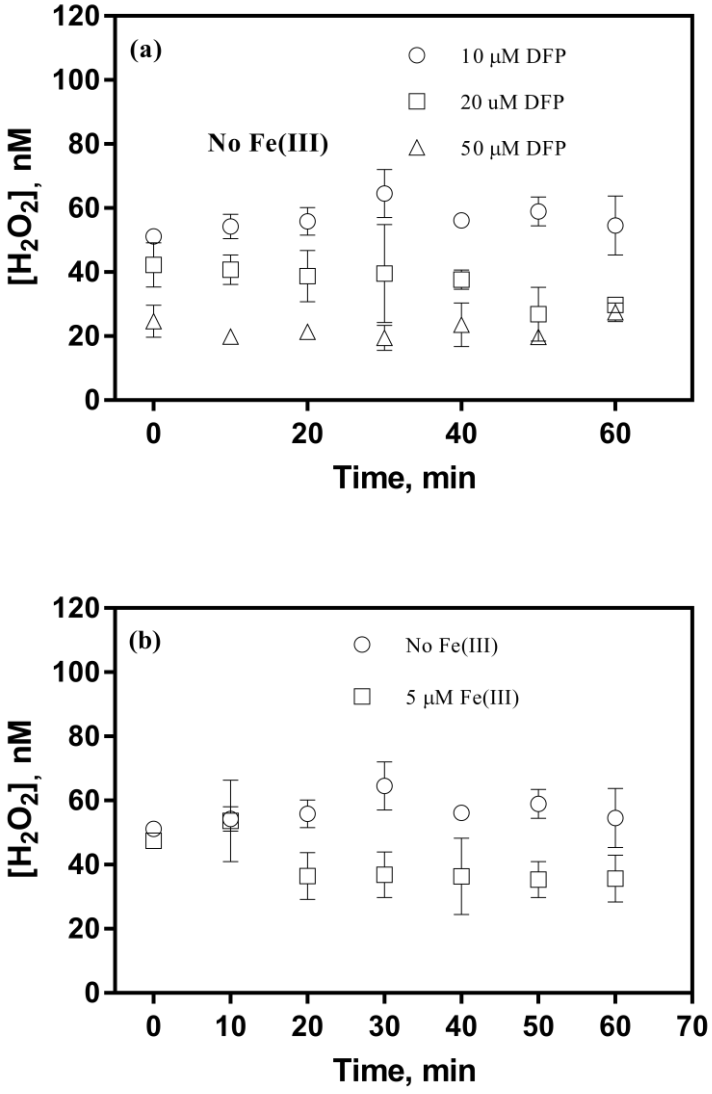

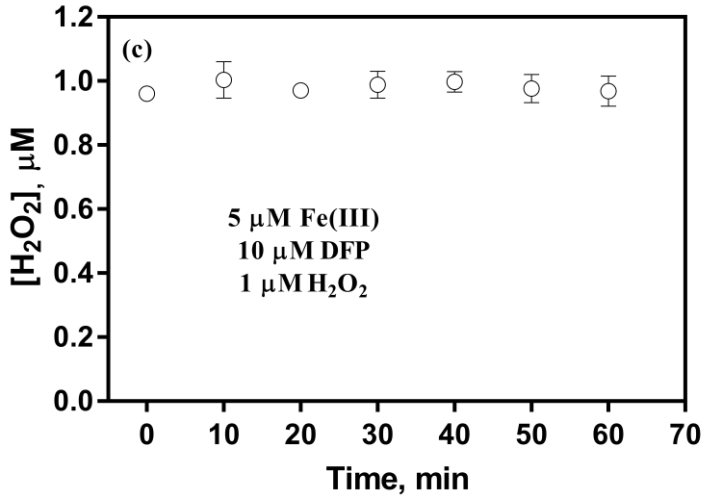

Figure S4 Measurement of H_2O_2 in the presence of (○) 10 μM, (□) 20 μM and (Δ) 50 μM DFP (panel a); in 10 μM DFP containing solutions with (○) no Fe(III) and (□) 5 μM Fe(III) (panel b) and in the presence of 5 μM Fe(III), 10 μM DFP and 1 μM H_2O_2 (panel c) at pH 7.4 in 0.1 M air-saturated NaCl solutions. Error bars are standard errors from duplicate measurements.

SI 5 Effect of DFP on the production of DA *o*-quinone (DAQ)

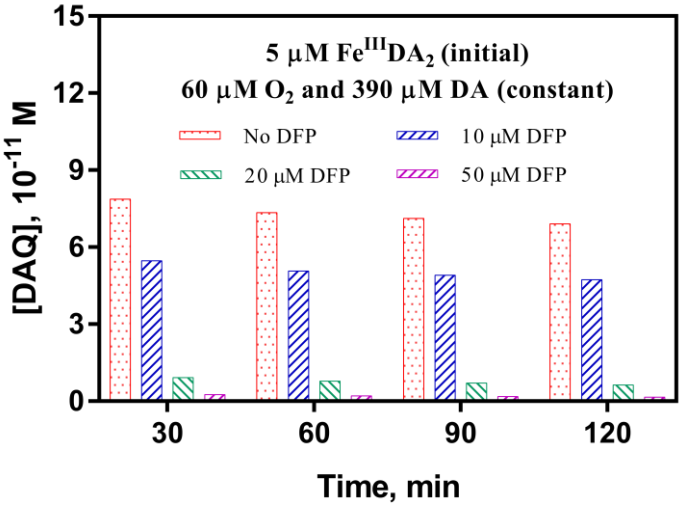

Figure S5. Effect of DFP on the generation of DAQ in the presence of 5 μM $Fe^{III}DA_2$ and constant concentrations of O_2 and DA.

SI 6 Materials and Methods

All analytical grade chemicals were purchased from Sigma-Aldrich (or as otherwise stated) and were used without further refinement. All solutions were prepared using 18 MΩ.cm ultrapure Milli-Q water (MQ). All glassware was acid washed in 5% (v/v) HCl for at least one week before use. Stock solutions were kept in dark bottles and were refrigerated at 4 ^{o}C when not in use. All experiments were conducted under dark conditions and performed at a controlled room temperature of 22 ± 0.6 ^{o}C.

Solutions were prepared at pH 7.4 by adding an appropriate amount of concentrated NaOH and HCl to buffer solutions containing 0.1 M NaCl, 2 mM $NaHCO_3$ and 10 mM HEPES (4-(2-Hydroxyethyl)piperazine-1-ethanesulfonic acid) buffer solution. All pH measurements were conducted using a Hanna HI9025 pH meter combined with a glass electrode and Ag/AgCl reference. Calibration of the pH electrode was undertaken using NIST buffer solutions (pH 7.01 and 10.01). Experiments were conducted in darkness with the reactor covered in foil for the duration of the reaction.

A concentrated Fe(II) stock solution (5 mM) was prepared by dissolving ferrous ammonium sulfate hexahydrate ($Fe(NH_4SO_4)_2 \cdot 6H_2O$) in 10 mM HCl. Concentrated stock solutions of 10 mM Fe(III) (using ferric chloride hexahydrate ($FeCl_3 \cdot 6H_2O$), 10 mM deferiprone (DFP) and 10 mM dopamine (DA) were prepared weekly in 10 mM HCl. The working stock solutions of Fe(II), Fe(III), DFP and DA were diluted from the concentrated stock solutions daily in 10 mM HCl. The acidity of both concentrated stock and working stock solutions was sufficient to avoid significant oxidation of Fe(II), DFP and DA and precipitation of Fe(III) on the time scale of interest and yet low enough to minimize any pH change that might occur on addition of the stock to experimental solutions. A stock solution of 20 mM H_2O_2 prepared by dilution of a nominal 30% (w⁄w) H_2O_2 solution was used for calibration of the H_2O_2 measurements. The nominal 30% w⁄w solution was standardized by UV spectrophotometry at 240 nm.[26] Concentrated stock solutions of 80 mM ferrozine (FZ) and 20 mM desferrioxamine B (DFB) were prepared in MQ. A daily prepared mixture containing 50 mM FZ and

5 mM DFB was used for Fe(II) determination. Stock solutions of 6 mM DPD (N,N-diethyl-*p*-phenylenediamine) and 500 KU/L HRP (horseradish peroxidase) were prepared in MQ water as described in previous work.[27] A 10 mM stock solution of DTPA (diethylenetriaminepentaacetic acid) was prepared in 10 mM HEPES and the pH was adjusted to 6.0. Stock solution of 20 mM 2,2′-bipyridyl was prepared in 5 mM HCl. The working solution of $Fe^{III}DA_2$ was prepared under deoxygenated condition. Specifically, in orders to prevent the oxidation of DA, the buffer solution (pH 7.4) used herein was sparged by using a special gas mixture of 297 ± 6 ppm CO_2 in argon (BOC) prior to the addition of 400 µM DA. The solution was then bubbled for another 10 min before the addition of Fe(III) to remove the possible O_2 existing in DA solution. To guarantee the complete formation of the $Fe^{III}DA_2$ complex, the DA and Fe(III) containing working solution was bubbled for at least 1 hour before the addition of DFP.

Measurement of Fe(II) concentration

The concentration of Fe(II) was quantified spectrophotometrically using the modified FZ method [28] in a 1 cm cuvette. The measurement was performed by a Cary 60 spectrophotometer at 562 nm with baseline correction at 690 nm. FZ was chosen because it reacts extremely rapidly with Fe(II) to form a stable purple complex ($Fe^{II}FZ_3$) with a maximum absorbance at 562 nm and molar absorptivity of $\varepsilon_{562\ nm}$ = 30,000 $M^{-1}cm^{-1}$.[29, 30] However, in the presence of organic complexing agents, FZ can facilitate reduction of both free and organically complexed Fe(III) resulting in over prediction of Fe(II) concentration in the samples. Thus, 200 µl DFB containing mixture was added into 2.5 ml sample solution to minimize reduction of both non- and organic bound Fe(III). Another advantage of the addition of DFB into iron and DFP containing solutions is that DFB can decompose the iron-DFP complexes by forming stable complexes with iron, which can eliminate of the influence of iron-DFP complexes on the absorbance at 562 nm. Since a small amount of Fe(III) was reduced by FZ even in the presence of DFB and contribute to the absorbance at 562 nm, in addition to the calibration of Fe(II), calibration of Fe(III) was also conducted. The concentration of Fe(II) was then calculated using the equation reported previously.[28]

$$[\mathrm{Fe(II)}] = \frac{A_{562} - \varepsilon_{\mathrm{Fe(III)}}[\mathrm{Fe}]_T}{\varepsilon_{\mathrm{Fe(II)}} - \varepsilon_{\mathrm{Fe(III)}}} \quad \text{S3}$$

Where A_{562} represents absorbance at 562 nm, $\varepsilon_{Fe(II)}$ represents molar absorption coefficient of $Fe^{II}FZ_3$ at 562 nm, $\varepsilon_{Fe(III)}$ represents the molar absorption coefficient of the small amount of $Fe^{II}FZ_3$ formed by reduction of Fe(III) in the presence of FZ, and $[Fe]_T$ represents the total Fe concentration.

Measurement of H_2O_2 concentration

The effect of DFP on the generation of H_2O_2 both in the absence and presence of iron and DA was quantified using the modified DPD method.[2, 27] Briefly, DPD is oxidized by H_2O_2 in the presence of HRP, resulting in the generation of DPD radicals. The generated DPD radicals are a function of H_2O_2 concentration. In general, DPD radicals have two typical peaks at both 551 nm and 510 nm with molar extinction coefficients at these wavelengths of 21,000 ± 500 $M^{-1}cm^{-1}$ and 19,800 ± 500 $M^{-1}cm^{-1}$, respectively. In order to decompose the iron-DFP complex and halt the possibly continuous generation of H_2O_2 during the measurement, 1.5 ml of 10 mM DTPA was added into 4 ml sample solution for its strong affinity for iron as a hexadentate chelator ($\log K_{Fe(III)+DTPA} = 28$).[31, 32] The system was calibrated by adding standard H_2O_2 stock into 4 ml buffer solutions and 1.5 ml DTPA stock solutions, along with a zero standard containing 60 µl of 6 mM DPD stock solution and 60 µl of 100 KU/L HRP. The calibration was constructed by linear regression of the calibration data. Interference arising from the presence of DFP and iron-DFP complex was found to be negligible under the experimental conditions investigated herein (shown in Figure S6). Given the influence of Fe(II) on the measurement for the scavenging of DPD radicals, in contrast to the system containing Fe(III), DFP and/or DA, another 500 µl of 20 mM 2,2′-bipyridyl was added into the system only containing Fe(II) and DFP before the addition of DTPA to bound any Fe(II) not being oxidized. The calibration of this system was undertaken by using the difference in the absorbance before and after adding DPD and HRP. Interference arising from the presence of Fe(III) and DFP was found to be negligible under the experimental conditions investigated herein (shown in Figure S7).

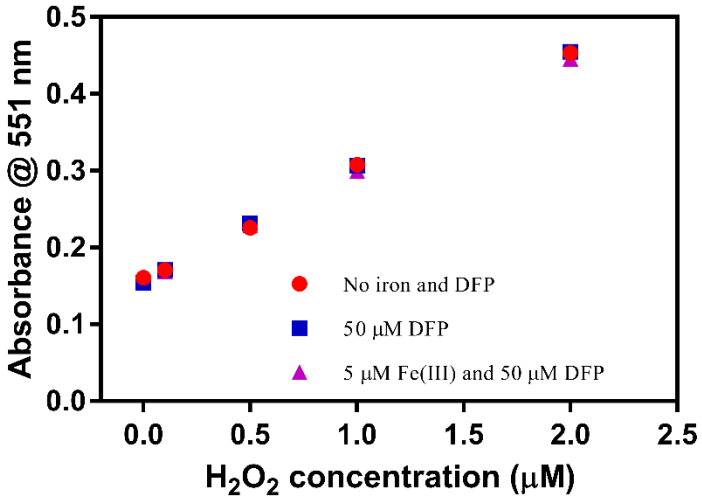

Figure S6 Measured absorbance of H_2O_2 at 551 nm with baseline correction at 690 nm in 0.1 M NaCl at pH 7.4 in 10 cm cuvette (●) in the absence of iron and DFP, (■) in the presence of 50 μM DFP and (▲) in the presence of 5 μM Fe(III) and 50 μM DFP. Some of the error bars are too small to be visible.

Figure S6 indicated that the presence of DFP and iron-DFP complex does not exert influence on the measurement of H_2O_2.

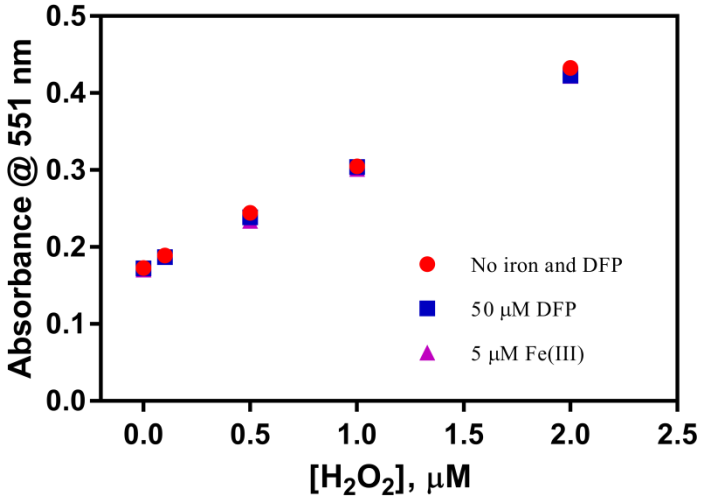

Figure S7 Measured absorbance of H_2O_2 at 551 nm in the presence of 6.25 µM Fe(II) with baseline correction at 690 nm in 0.1 M NaCl at pH 7.4 (●) in the absence of DFP and Fe(III) and (■) in the presence of 50 µM DFP and (▲) 5 µM Fe(III). Error bars are standard errors from duplicate measurements, some of which are too small to be visible.

Figure S7 indicated that the presence of moderate concentrations of Fe(III) (5 µM) and DFP (50 µM) does not have significant influence on the measurement of H_2O_2 in the presence of 6.25 µM Fe(II) and high concentrations of 2,2′-bipyridyl.

Measurement of $Fe^{III}DFP_3$ complex

As a bidentate chelator, DFP is expected to form three different kinds of complexes with Fe(III): the *mono*-complex (referred to hereafter as $Fe^{III}DFP$, $\varepsilon_{575\ nm}$ ~ 2,000 $M^{-1}cm^{-1}$), the *bis*-complex (referred to hereafter as $Fe^{III}DFP_2$, $\varepsilon_{516\ nm}$ ~ 3,000 $M^{-1}cm^{-1}$) and the *tris*-complex (denoted hereafter as $Fe^{III}DFP_3$, $\varepsilon_{450\ nm}$ ~ 4,600 $M^{-1}cm^{-1}$) with the dominant species being pH and concentration-dependent.[18, 33] Details of the distribution of different complexes can be found in the section SI 3.

The concentration of $Fe^{III}DFP_3$ was determined spectrophotometrically by measuring the peak absorbance at 460 nm which is close to the published value.[18, 33, 34] The measurement was conducted by using a Cary 60 spectrophotometer with baseline correction undertaken at 800 nm. Calibration curves for quantification of the concentration of the $Fe^{III}DFP_3$ complex were developed under deoxygenated conditions to prevent any possible transformation of the complex. The spectrum and calibration curves were shown in Figure S8 below. The molar absorptivity of $Fe^{III}DFP_3$ was calculated to be 4,871 $M^{-1}cm^{-1}$, which is close to the previously published value of 4,600 $M^{-1}cm^{-1}$.

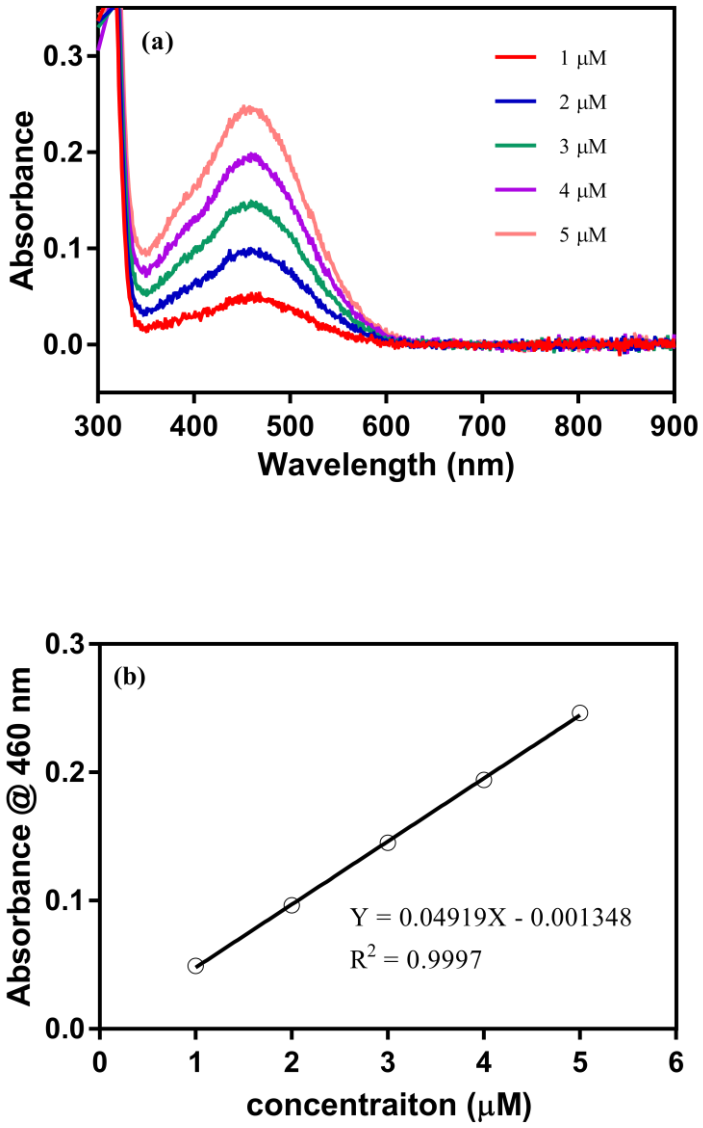

Figure S8. Measured spectrum of $Fe^{III}DFP_3$ complexes (panel a) and calibrations for $Fe^{III}DFP_3$ complexes (panel b) in 0.1 M NaCl at pH 7.4 in the presence of 500 µM DFP under deoxygenated condition.

Reference

[1] Morel, F. M., and Hering, J. G. (1993) *Principles and applications of aquatic chemistry*, Wiley, New York.

[2] Sun, Y., Pham, A. N., and Waite, T. D. (2016) Elucidation of the interplay between Fe(II), Fe(III), and dopamine with relevance to iron solubilization and reactive oxygen species generation by catecholamines, *J Neurochem 137*, 955-968.

[3] Pham, A. N., and Waite, T. D. (2014) Cu (II)-catalyzed oxidation of dopamine in aqueous solutions: Mechanism and kinetics, *J Inorg Biochem 137*, 74-84.

[4] Borovansky, J., Edge, R., Land, E. J., Navaratnam, S., Pavel, S., Ramsden, C. A., Riley, P. A., and Smit, N. P. (2006) Mechanistic studies of melanogenesis: the influence of *N* - substitution on dopamine quinone cyclization, *Pigm Cell Res 19*, 170-178.

[5] Land, E., Ito, S., Wakamatsu, K., and Riley, P. (2003) Rate constants for the first two chemical steps of eumelanogenesis, *Pigm Cell Res 16*, 487-493.

[6] Zafiriou, O. C. (1990) Chemistry of superoxide ion-radical (O_2^-) in seawater. I. pK^*_{aswb} (HOO) and uncatalyzed dismutation kinetics studied by pulse radiolysis, *Mar Chem 30*, 31-43.

[7] Pham, A. N., Rose, A. L., Feitz, A. J., and Waite, T. D. (2006) Kinetics of Fe(III) precipitation in aqueous solutions at pH 6.0–9.5 and 25°C, *Geochim Cosmochim Acta 70*, 640-650.

[8] Blesa, M. A., and Matijević, E. (1989) Phase transformations of iron oxides, oxohydroxides, and hydrous oxides in aqueous media, *Adv Colloid Interfac 29*, 173-221.

[9] El-Avaan, U., Herlinger, E., Jameson, R., and Linert, W. (1997) Anaerobic oxidation of dopamine by iron(III), *J Chem Soc, Dalton Trans 16*, 2813-2818.

[10] Rush, J. D., and Bielski, B. (1985) Pulse radiolytic studies of the reactions of $HO_2/O_2^-$with Fe(II)/Fe(III) ions. The reactivity of HO_2/O_2^- with ferric ions and its implication on the occurrence of the Haber-Weiss reaction, *J Phys Chem 89*, 5062-5066.

[11] González-Davila, M., Santana-Casiano, J. M., and Millero, F. J. (2005) Oxidation of iron (II) nanomolar with H_2O_2 in seawater, *Geochim Cosmochim Acta 69*, 83-93.

[12] Ludwig, C., Casey, W. H., and Rock, P. A. (1995) Prediction of ligand-promoted dissolution rates from the reactivities of aqueous complexes, *Nature 375*, 44-47.

[13] Rose, A. L., and Waite, T. D. (2003) Kinetics of iron complexation by dissolved natural organic matter in coastal waters, *Mar Chem 84*, 85-103.

[14] King, D. W. (1998) Role of carbonate speciation on the oxidation rate of Fe (II) in aquatic systems, *Environ Sci Technol 32*, 2997-3003.

[15] Millero, F. J., and Hawke, D. J. (1992) Ionic interactions of divalent metals in natural waters, *Mar Chem 40*, 19-48.

[16] Smith, R. M., and Martell, A. E. (1989) *Critical stability constants, Vol. 6: Second Supplement*, Vol. 6, Plenum Press, New York, USA.

[17] Merkofer, M., Domazou, A., Nauser, T., and Koppenol, W. H. (2006) Dissociation of CP20 from Iron(II)$(cp20)_3$: A pulse radiolysis study, *Eur J Inorg Chem 2006*, 671-675.

[18] Merkofer, M., Kissner, R., Hider, R. C., and Koppenol, W. H. (2004) Redox properties of the iron complexes of orally active iron chelators CP20, CP502, CP509, and ICL670, *Helv Chim Acta 87*, 3021-3034.

[19] Avdeef, A., Sofen, S. R., Bregante, T. L., and Raymond, K. N. (1978) Coordination chemistry of microbial iron transport compounds. 9. Stability constants for catechol models of enterobactin, *J Am Chem Soc 100*, 5362-5370.

[20] Motekaitis, R. J., and Martell, A. E. (1991) Stabilities of the iron(III) chelates of 1, 2-dimethyl-3-hydroxy-4-pyridinone and related ligands, *Inorg Chim Acta 183*, 71-80.

[21] Millero, F. J., Yao, W., and Aicher, J. (1995) The speciation of Fe (II) and Fe (III) in natural waters, *Mar Chem 50*, 21-39.

[22] Schecher, W. D., and McAvoy, D. C. (1992) MINEQL+: a software environment for chemical equilibrium modeling, *Comput Environ Urban Syst 16*, 65-76.

[23] Sun, Y., Pham, N., and Waite, D. (2018) The effect of Vitamin C and iron on dopamine-mediated free radical generation: implications to Parkinson's Disease, *Dalton Trans* DOI: 10.1039/C7DT04373B.
[24] Miller, D. M., Buettner, G. R., and Aust, S. D. (1990) Transition metals as catalysts of "autoxidation" reactions, *Free Radical Bio Med 8*, 95-108.
[25] Duesterberg, C. K., and Waite, T. D. (2006) Process optimization of Fenton oxidation using kinetic modeling, *Environ Sci Technol 40*, 4189-4195.
[26] Morgan, M. S., Van Trieste, P. F., Garlick, S. M., Mahon, M. J., and Smith, A. L. (1988) Ultraviolet molar absorptivities of aqueous hydrogen peroxide and hydroperoxyl ion, *Anal Chim Acta 215*, 325-329.
[27] Bader, H., Sturzenegger, V., and Hoigne, J. (1988) Photometric method for the determination of low concentrations of hydrogen peroxide by the peroxidase catalyzed oxidation of N, N-diethyl-*p*-phenylenediamine (DPD), *Water Res 22*, 1109-1115.
[28] Garg, S., Ito, H., Rose, A. L., and Waite, T. D. (2013) Mechanism and kinetics of dark iron redox transformations in previously photolyzed acidic natural organic matter solutions, *Environ Sci Technol 47*, 1861-1869.
[29] Stookey, L. L. (1970) Ferrozine - a new spectrophotometric reagent for iron, *Anal Chem 42*, 779-781.
[30] Viollier, E., Inglett, P., Hunter, K., Roychoudhury, A., and Van Cappellen, P. (2000) The ferrozine method revisited: Fe (II)/Fe (III) determination in natural waters, *Appl Geochem 15*, 785-790.
[31] Martell, A. E., and Smith, R. M. (1974) *Critical stability constants, Vol. 1*, Vol. 1, Plenum Press, New York, USA.
[32] Engelmann, M. D., Bobier, R. T., Hiatt, T., and Cheng, I. F. (2003) Variability of the Fenton reaction characteristics of the EDTA, DTPA, and citrate complexes of iron, *Biometals 16*, 519-527.
[33] Nurchi, V. M., Crisponi, G., Pivetta, T., Donatoni, M., and Remelli, M. (2008) Potentiometric, spectrophotometric and calorimetric study on iron (III) and copper (II) complexes with 1, 2-dimethyl-3-hydroxy-4-pyridinone, *J Inorg Biochem 102*, 684-692.
[34] Devanur, L. D., Evans, R. W., Evans, P. J., and Hider, R. C. (2008) Chelator-facilitated removal of iron from transferrin: relevance to combined chelation therapy, *Biochem J 409*, 439-447.